Structural basis of NKT cell inhibition using the T-cell receptor-blocking anti-CD1d antibody 1B1*

Ge Ying[1], Jing Wang[1], Thierry Mallevaey[2,3], Serge Van Calenbergh[4], and Dirk M. Zajonc[1,5,#]

[1]Division of Immune Regulation, La Jolla Institute for Immunology, La Jolla, California 92037, USA.

[2]Department of Immunology, University of Toronto, Toronto, Ontario M5S 1A8, and [3]Institute of Biomaterials and Biomedical Engineering, University of Toronto, Toronto, Ontario M5S 3G9, Canada.

[4]Laboratory for Medicinal Chemistry (FFW), Faculty of Pharmaceutical Sciences, and [5]Department of Internal Medicine, Faculty of Medicine and Health Sciences, Ghent University, 9000 Ghent, Belgium.

*Running title: *Structure of the mouse CD1d/1B1-Fab complex*

[#]To whom correspondence should be addressed: Dirk M. Zajonc, E-mail: Dirk.Zajonc@pfizer.com
Cancer Immunology Discovery, Pfizer, San Diego, CA 92121, USA.

Keywords: antibody, glycolipid, antigen presentation, major histocompatibility complex (MHC), T-cell receptor (TCR), cellular immune response, natural killer T cell activation, 1B1 Fab, immune signaling

ABSTRACT

Natural killer T (NKT) cells are a subset of T lymphocytes that recognize glycolipid antigens presented by CD1d molecule (CD1d). They rapidly respond to antigen challenge and can activate both innate and adaptive immune cells. To study the role of antigen presentation in NKT cell activation, previous studies have developed several anti-CD1d antibodies that block CD1d binding to T-cell receptors (TCRs). Antibodies that are specific to both CD1d and the presented antigen can only be used to study the function of only a limited number of antigens. In contrast, antibodies that bind CD1d and block TCR binding regardless of the presented antigen can be widely used to assess the role of TCR-mediated NKT cell activation in various disease models. Here, we report the crystal structure of the widely used anti-mouse CD1d antibody 1B1 bound to CD1d at a resolution of 2.45Å and characterized its binding to CD1d-presented glycolipids. We observed that 1B1 uses a long hydrophobic H3 loop that is inserted deep into the binding groove of CD1d where it makes intimate non-polar contacts with the lipid backbone of an incorporated spacer lipid. Using an NKT cell agonist that has a modified sphingosine moiety, we further demonstrate that 1B1 in its monovalent form cannot block TCR mediated NKT cell activation, since 1B1 fails to bind with high affinity to mCD1d. Our results suggest potential limitations of using 1B1 to assess antigen recognition by NKT cells, especially when investigating antigens that do not follow the canonical two-alkyl-chain rule.

Besides a role in immunotherapies, antibodies that block receptor-ligand interactions are often used to assess the importance of a specific signaling axis in immune activation or inhibition. Receptor-ligand interactions can be complex and often involve more than two molecules. For example, T cells use their antigen receptor (TCR) to recognize the ligand, which forms a composite epitope formed by the antigen-presenting molecule Major Histocompatibility Complex (MHC) and the small antigen that it presents (1). Therefore, antibodies that block TCR engagement of MHC molecules ideally have an overlapping binding site with the TCR on the MHC molecule. Antibodies that block TCR mediated T cell activation exist for all MHC molecules including MHC class I (2-5),

MHC class II (6), and CD1d (7-9) and are widely used to study or modulate T cell function by specifically blocking antigen-mediated TCR activation. While some antibodies are specific for the MHC molecule and the antigen, such as the NKT cell antigen receptor blocking antibody L363 that recognizes mouse (m)CD1d presenting α-galactosylceramide (αGalCer), the anti-mCD1d antibody 1B1 binds to mCD1d regardless of the presented antigen (9).

Natural Killer T (NKT) cells are a population of T lymphocytes that recognize glycolipid antigens presented by the non-classical MHC I homolog CD1d. NKT cells are activated within hours after antigen-stimulation and rapidly produce both pro- and anti-inflammatory cytokines (10). Type I and Type II NKT cells are the major classes of NKT cells, and they differ in both their TCR usage and their antigen-specificity (11). Type I NKT cells express a semi-invariant αβ T cell receptor (TCR) alpha chain (Vα14Jα18 in mouse, Vα24Jα18 in humans) that pairs with a limited number of TCR β chains (Vβ8.2, and to a lesser extend Vβ7 and Vb2 in mouse, Vβ11 in human) (10,12). The prototypical antigen α-galactosylceramide (αGalCer) is the common antigen for Type I NKT cells (13). Type II NKT cells do not have a conserved TCR rearrangement and do not recognize a common antigen, making them difficult to identify and characterize. While Type II NKT cells can recognize a variety of different antigens, a well-characterized and major subset recognizes sulfatide self-antigens (14-17).

In addition to Type I and Type II NKT cells, minor subsets of unconventional NKT cells have also been identified and structurally characterized. While these NKT cells exhibit specificity toward αGalCer, or related glycolipids the TCR repertoire is markedly different from the conventional Type I NKT cells (18,19).

Glycolipids are bound by CD1d with the lipid backbone deeply inserted into a hydrophobic binding groove that is composed of two major pockets, A′ and F′. Each pocket accommodates one alkyl chain of a dual alkyl chain lipid. For ceramide-based lipids, such as αGalCer or sulfatide, the acyl chain is accommodated in the larger A′ pocket, while the sphingosine moiety is bound in the F′ pocket (20-22). The binding orientation of diacylglycerolipids is less restricted and the *sn*-1 and *sn*-2 linked acyl chain can go in either of the two pockets, depending on number and positions of unsaturations located within the fatty acyl chains (23-28). The different headgroups of the various glycolipids are exposed at or above the CD1d binding groove for TCR recognition.

NKT cells generally recognize the exposed headgroup and a few polar groups of the lipid backbone. Type I NKT cells maintain a conserved binding footprint centered over the F′ pocket of CD1d, while the sulfatide-restricted Type II NKT cell clone XV19 binds over the A′ pocket (29-33). Both TCRs contact their antigens from the side with only one chain, TCRα for Type I and TCRβ for Type II NKT cells. There is no overlap in the mCD1d binding footprint between Type I NKT cells and the XV19 Type II NKT cell clone. The anti-mCD1d antibody 1B1 is able to block both TCR mediated activation of Type I and Type II NKT cells (ref), suggesting it has an overlapping binding site with the TCRs from both NKT cell subsets. However, since the glycolipid is presented in the center of the CD1d binding groove between both TCR binding sites this raises the questions as to how 1B1 is able to bind mCD1d and compete with both TCRs, while not being impacted by the presented glycolipid.

In order to understand how 1B1 binds to mCD1d and blocks both Type I and Type II NKT cell activation, we assessed the binding of 1B1 to CD1d presenting different glycolipids using Surface Plasmon Resonance studies. We have further assessed the ability of 1B1 Fab and 1B1 IgG in blocking Type I and Type II NKT cell responses toward different lipid antigens and determined the crystal structure of 1B1 Fab bound to mCD1d at a resolution of 2.45Å.

RESULTS

Generation of 1B1 Fab and mCD1d for structural studies-We have generated 1B1 Fab by papain digestions and formed complexes with insect cell expressed mCD1d that was either loaded with α-GalCer or not incubated with a particular lipid. While we were able to obtain crystals of the complex, we were not able to obtain a diffraction dataset beyond 3.9 Å. Therefore, we have generated 1B1 Fab recombinantly in SF9 insect cells, to limit heterogeneity introduced during the papain digestion. We have further generated mCD1d via refolding to avoid the presence of N-linked glycans. Since mCD1d contains an unpaired cysteine at the bottom of the A′ pocket (Cys12), we first replaced this residue against serine (mCD1d C12S). We formed complexes of all possible combinations of the 4 proteins (2 Fab and 2 mCD1d) and finally obtained high quality diffracting crystals for the

complex consisting of refolded mCD1d and the insect cell expressed 1B1 Fab.

1B1 Fab-mCD1d crystal structure-To determine the structural basis of how 1B1 blocks NKT cell activation, we have determined the crystal structure of the 1B1 Fab/mCD1d complex to 2.45Å resolution (Table 1, Fig. 1). CD1d forms the typical heterodimeric arrangement in which the CD1d heavy chain non-covalently associates with β2-microglobulin. However, since CD1d has been refolded, no N-linked glycans are present in the structure. In addition, during the course of refolding, three spacer molecules have been incorporated into CD1d to stabilize the hydrophobic pocket. Two molecules are incorporated into the larger A′ pocket and one into the F′ pocket of CD1d (Figure 1). Based on the extent of the observed electron density, we modeled three C16 alkyl chains, which mimic the position of the alkyl chains generally associated with glycolipid antigens (Figure 2).

The 1B1 Fab binds perpendicular across the lipid binding groove of mCD1d, centered above the F′ pocket. The majority of contacts are formed between the H chain and CD1d. The H chain uses 575 $Å^2$ and the L chain 45 $Å^2$ of protein surface and together they contact 610 $Å^2$ of CD1d (Table 2). A single contact is formed between CDR L1 residue Tyr31 and CD1d Glu83, while the H chain binding is dominated by hydrophobic contacts (Table 3). Only H2 and H3 participate in CD1d binding and in together they form three hydrogen bonds and two salt bridges. H2:Asp55 forms both a salt bridge and H bond with Lys148 of CD1d, while H3:Arg109 forms a salt bridge with Asp 80 of CD1d, H3:Gly105 a H bond with Asp153, and Leu106 a H bond with Asp80. A characteristic feature of the interaction between 1B1 Fab and CD1d is an elongated H3 loop that inserts into the F′ pocket of CD1d like a hydrophobic finger and forms many hydrophobic contacts with surrounding CD1d residues (Fig 1 and 2, Table 3). The H3 loop has two tyrosine residues (Tyr103 and Try104) that extend outward and slightly upwards from this finger and together appear to dictate how far the loop inserts into the binding groove of CD1d (Figure 2B). Surprisingly, the H3 loop also is in close contact with one of the spacer molecules that mimics the position of the sphingosine chain of glycolipids, such as sulfatide or α-GalCer (Figure 2). H3:Tyr104, Gly105, and Leu106 each form one VDW contact with the spacer lipid, but the overall intimate binding position of H3 leads to a combined total buried surface interface of 212 $Å^2$.

1B1 Fab binding kinetics- When we superimpose the 1B1/mCD1d complex with that of mCD1d/sulfatide (PDB ID 2AKR (20)), we notice that the H3 loop of 1B1 is very close to sulfatide, especially to the C4"-OH of the galactose (Figure 2B). Therefore, we wanted to test the impact of 1B1 binding to CD1d that presents glycolipids with different sizes of headgroups. We chose sulfatide and GT1b as model antigens, since they are negatively charged and their loading efficiency can be visualized. Since 1B1 binds to CD1d without presenting a given lipid, we needed to achieve a near to 100% loading efficiency to avoid having an overlapping binding response contributed by unloaded CD1d molecules. After glycolipid loading, both sulfatide and GT1b bind to 100% to CD1d (Figure 2C) and we used these complexes for surface plasmon resonance studies with the 1B1 Fab (Figure 3D). However, the binding affinity of 1B1 to mCD1d is nearly identical in all three analyzed CD1d-lipid complexes, suggesting that variations in the glycolipid headgroups can be accommodated by 1B1 and do not affect its binding affinity toward CD1d. 1B1 Fab binds with a KD of ~12.5 nM calculated from an association rate (kon) of 5.4-6.1 x 10^5 and a dissociation rate (koff) of 6.2-7.3 x 10^{-3} (Figure 2C).

Comparison between 1B1 and the TCR of iNKT cells- When we compared the binding site of 1B1 with that of the Vα14Vβ8.2 TCR of iNKT cells, we noticed a similar footprint on CD1d (Figure 1E, 3, and 4). While 1B1 binds perpendicular across the F′ pocket of CD1d, the TCR binds parallel along both α-helices (Figure 1E). In addition, while TCR binding seems to be dominated by the CDR3α region, 1B1 uses its elongated H3 loop to form the majority of contacts. In both molecules, a hydrophobic finger, Leu99α of the TCR and $Leu106_H$ of the antibody, binds at the F′ pocket of CD1d. In striking contrast, however, 1B1 inserts its hydrophobic finger much deeper into the F′ pocket, compared to the TCR (Figure 3A). That results in a different binding mode. While the TCR sits above the F′ pocket and binds to the F′ roof, the antibody prevents F′ roof formation and instead sits as a wedge inside the F′ pocket (Figure 2 B-D). In fact, CDR3α of the TCR flattens out at the tip and hovers above CD1d, while the H3 loop is straight and reaches into the CD1d binding groove (Figure 3C, D). The deep location of the H3 loop raises the question as to whether the nature of the lipid chain that is bound inside the F′ pocket can impact 1B1 binding. While common dual alkyl-

chain based lipids, such as α-GalCer are nestled underneath $Leu106_H$ of 1B1, lipids containing modifications could potentially impact 1B1binding. We chose a modified lipid αGSA[26,P5*p*], and superimposed its crystal structure (PDB ID 6C6F) with the CD1d/1B1 structure. $Leu106_H$ is very close to the phenyl group contained in the modified sphingamide chain (2.4Å).

1B1 blocking of Type I and Type II NKT cell activation- We then analyzed the ability of 1B1 (both Fab and IgG) to block NKT cell activation by various glycolipids. We loaded antigens for both Type I and Type II NKT cells into mCD1d and performed a NKT cell hybridoma activation assay using the NKT hybridomas 1.2 (Type I) and XV19 (Type II) in the presence or absence of the TCR blocking antibody 1B1 (Figure 4). A 1B1 dose titration demonstrated that the activation of both Type I and Type II NKT cells by α-GalCer and sulfatide can be fully blocked with both 1B1 Fab and 1B1 IgG. 1B1 Fab appears to block Type I NKT cell activation at a lower dose (15.6 μg/ml) compared to Type II NKT cells (100 μg/ml), while 1B1 IgG blocks both hybridoma activation at the lowest dose used in this assay (1.5 μg/ml, equivalent to equimolar ratio with CD1d). Using a structure-guided approach, we generated the 1B1 Fab Y103K/I56S double mutant, which does not bind mouse or human CD1d (Figure 2). The 1B1 mutant is unable to block NKT cell activation as expected (Figure 4). However, using the modified sphingamide antigen αGSA[26,P5*p*], we noticed that 1B1 Fab is unable to block NKT cell activation, suggesting that the 1B1 binding affinity to mCD1d is greatly reduced when αGSA[26,P5*p*] is bound, due to steric clashes with the elongated H3 loop and the phenyl moiety of the ligand. Since we could not load αGSA[26,P5*p*] to mCD1d at 100%, we were unable to precisely measure the 1B1 binding kinetics via SPR. Our data suggests the reduced binding affinity drops below a threshold necessary for blocking NKT cell responses. This is evident when using 1B1 IgG, which in its natural bivalent form has an increased binding avidity. 1B1 IgG is fully able to block NKT cell activation by αGSA[26,P5*p*]. This demonstrated that while common NKT cell antigens can be blocked by 1B1, one must be mindful when using 1B1 to block NKT activation of structurally diverse glycolipids, such as cholesterol antigens or hydrophobic peptides, which do not follow the dual alkyl chain rule.

DISCUSSION

In this study we have determined the crystal structure of the 1B1 Fab bound to mouse CD1d. 1B1 binds to mCD1d in a perpendicular binding orientation across the F' pocket, directly overlapping with the binding site of the TCR of iNKT cells but with minimal overlap with the binding site of the Type II NK TCR clone XV19 that binds above the A′ pocket of CD1d (31,34-37). Nevertheless, 1B1 blocks TCR mediated activation of both Type I and Type II NKT cells, as 1B1 overlaps with XV19 TCR in the central region between the A′ and F′ pocket. 1B1 is more potent in inhibiting Type II NKT cell responses correlating with a greatly reduced binding affinity of the XV19 TCR compared to the Vα14Vβ8.2 TCR of Type I NKT cells. The XV19 TCR binds with micromolar affinity (K_D=6-24 μM) to CD1d-sulfatide, while the Vα14Vβ8.2 TCR binds with a K_D of 10-30 nM to CD1d-αGalCer complexes (28,30,32,33). The characteristic feature of 1B1 is its long H3 loop that inserts into the F′ pocket of CD1d, thereby preventing the closure of the F′ roof. The F′ roof is a hallmark and a major binding site for the CDR3α region of the Vα14Vβ8.2 TCR of Type I NKT cells. Since the H3 loop of 1B1 is deeply inserted into the CD1d groove, one side of the loop runs alongside the alkyl chain of a CD1d bound glycolipid. As alkyl chains generally do not differ greatly in structure for the various glycolipids, 1B1 binding is not affected by the nature of the presented lipid. However, when considering other ligands, such as the hydrophobic peptide p99 or a cholesterol antigen, 1B1 binding may be greatly impaired or even abrogated (38,39). We showed the influence of lipid modifications in 1B1 binding using the α−galactosylsphingamide antigen αGSA[26,P5*p*]. The 1B1 Fab is unable to prevent Type I NKT cell activation using this antigen, suggesting that the binding affinity of 1B1 to CD1d presenting αGSA[26,P5*p*] is reduced below a threshold necessary for competing with TCR binding. However, when the intact IgG is used, 1B1 is able to block activation, yet slightly less efficient. Together these data suggest that while 1B1 is a potent blocker of TCR mediated T cell activation for both Type I and Type II NKT cells, its binding strength to CD1d can be affected by the antigen that is presented by CD1d. This could result in a scenario where the activity of an antigen for NKT cells cannot be blocked by 1B1, leading to the incorrect assumption that the antigen activates NKT cells through a mechanism that does not involve TCR binding.

EXPERIMENTAL METHODS

Glycolipid Ags –Bovine brain sulfatides and GT1b were purchased from Avanti Polar Lipids Inc. C16 α-GalCer, α-GSA[26,P5*p*] and C24:1-sulfatide were synthesized as previously reported (40-42).

Cell line and cell culture - The hybridoma cell line expressing the rat anti-mouse IgG2b mAb 1B1 was grown in RPMI-1640 medium (Invitrogen, Carlsbad) supplemented with 10 mM HEPES pH 7.5, 1% L-glutamine, 1% nonessential amino acids, 1% Sodium Pyruvate 55 μM 2-mercaptoethanol, 20 μg/ml gentamicin (Gibco) and 10% heat-inactivated fetal calf serum (FCS). The hybridoma was maintained in an incubator with a humidified atmosphere containing 5% CO_2 at 37 ºC.

Antibody production and purification. The 1B1 hybridoma cells were gradually adapted to culture in protein-free hybridoma media (PFHM-II, Gibco), supplemented as indicated above. Cells from two T175 tissue culture flasks were transferred into one 2 L roller bottle, filled up to 1.5 L with supplemented PFHM-II. Roller bottles were equilibrated with CO_2 by placing in the 37ºC + 5% CO_2 incubator with the lid loosened for 1/2-1 hour, then grown with closed lid at 37º C while rolling for approximately 2 weeks or until the media turned yellow. Cells were spun down (1250 rpm for 6 min) and supernatant was filtered (0.22μm) and concentrated to 300ml using a tangential flow through filtration unit (Millipore, Pellicon 2) while exchanging buffer to PBS. IgG was collected from supernatant using affinity chromatography using a 5 ml HiTrap ProteinG column (GE Healthcare). IgG was eluted from the column with 0.1 M glycine pH 3.0, while 0.7 ml fractions were collected in 1.5 ml test tubes containing 0.3 ml of 1M Tris pH 8.5 for neutralization. IgG containing fractions were pooled and buffer exchanged against PBS using centrifugal filtration devices (Amicon Ultra, Millipore). Final yield of purified 1B1 IgG was 12 mg/L of culture.

Cloning and sequencing of 1B1 VH and VL genes – RNA isolation and sequencing was performed as reported previously for the α-GalCer specific mAb L363 (43), with some modifications including a poly-G tailing method (44). Briefly, total RNA was isolated from $5x10^6$ hybridoma cells using the RNeasy Mini kit (Qiagen) according to the manufacturer's instructions. First-strand cDNA synthesis of 5'RACE was performed according to the protocol for Clontech's SMART-RACE using the Clontech cDNA amplification kit and the Invitrogen SuperScript II Reverse Transcriptase at 42ºC for 50 min in a 20 μl reaction volume containing: 500 ng of total RNA, 0.6 μM 5'-RACE CDS Primer A, 0.6 μM SMART II A oligonucleotide, 1x RT buffer (20 mM Tris-HCl, pH 8.4, 50 mM KCl), 5 mM MgCl2, 0.01 M DTT and 4 U RNase out recombinant RNAse inhibitor. The first strand cDNA was then poly-G tailed using terminal deoxynucleotidyl transferase (TdT, 15U, Promega), 10 uM dGTP (GE healthcare), 1x reaction buffer (100 mM cacodylate buffer pH6.8, 1 mM CoCl2 and 0.1 mM DTT; Promega) at 37 °C for 1 h. The TdT was then heat inactivated at 70 °C for 10 min. The tailed cDNA was amplified by PCR using a sense primer containing poly-C sequence and a rat IgG specific anti-sense primer (second strand reaction). For the PCR reaction, 48 μl of PCR mix containing 1x PCR buffer, 1.5 mM MgCl2, 0.2 mM dNTP, 1 μM ANCTAIL sense primer 5'-cgtcgatgagctctagaattcgcatgtgcaagtccgatggtccccccc ccccccc-3', 1 μM ratκC643-rev antisense primer 5'-aggatgatgtcttatgaacaa-3', and 1.5 U high-fidelity Taq DNA polymerase were added to 2.5 μl cDNA (from the first-strand reaction) as suggested (45). The cycling profile used for the PCR was: denaturation at 94ºC for 30 seconds, annealing at 60ºC for 30 seconds, extension at 72ºC for 3 min. At the end of the 30 cycles, a 10 min incubation step at 72ºC was done to complete elongation. The resulting PCR products were cloned into the pGEM-T easy vector (Promega) for sequencing. The VJ and VDJ gene rearrangement was determined as IGKV9S1*01 F/ IGKJ2-3*01 F (light chain) and IGHV5-25*01 F, IGHJ1*01 F, and IGHD1-6*01 F (heavy chain) using the IMGT server (46).

Fab digestion and purification - Purified 1B1 mAb (rat IgG2b) at 1 mg/ml in PBS was incubated with 1 % (w/w) activated papain (Sigma #P3125) and for 3h at 37ºC in digestion buffer. Papain was activated by incubating 20 μl papain with 100 μl 10X papain buffer (1M NaOAc pH 5.5, 12 mM EDTA) and 100 μl cysteine (12.2 mg/ml) for 15 min at 37ºC. The papain digestion was stopped by adding 20 mM Iodoacetamide (IAA). Digestion mix was concentrated and adjusted to PBS for subsequent protein A purification to remove undigested IgG and Fc. The protein A flow-through containing Fab was dialyzed against 20 mM NaOAc pH 5.5 overnight and purified to homogeneity by cation-exchange chromatography using MonoS (GE Healthcare).

Mouse CD1d/β2m expression in insect cells - The expression and purification methods of fully glycosylated mouse CD1d/β2m heterodimer proteins using the baculovirus expression system were reported previously (31,34,47).

Gene cloning and site directed mutagenesis - cDNA of mouse CD1d (mCD1d) was subcloned into the *E. coli* expression vector pET-22b for subsequent expression in inclusion bodies. Single amino acid mutation C12S (TGC>TCC) was introduced into mCD1d using the Quick Change II site-directed mutagenesis kit (Stratagene) with primers C12S-forward (5'-GAATTACACCTTCCGCTCCCTGCAGATGTC TTCC-3') and C12S-reverse (5'-GGAAGACATCTGCAGGGAGCGGAAGGTGT AATTC-3'). Successful mutation was verified by sequencing. Mouse beta2-microblobulin (β2M) without leader peptide was cloned into a separate pET-22b vector. Synthetic DNA for wild type 1B1 Fab and the 1B1 Fab mutant Y103K/I56S, which is unable to bind to mCD1d, was synthesized by Genscript and sub-cloned into the dual promoter vector pBACpHp10 with a C-terminal hexa-histidine tag on the heavy chain and expressed in SF9 insect cells using the baculovirus expression system. SF9 cells were removed from the cell culture media by centrifugation, and the media was further concentrated to 0.3 liter and washed twice with PBS buffer. The protein was purified from the concentrated media by affinity chromatography on a Ni-NTA resin (Takara Bio.) in 50 mM Tris-HCl, 300 mM NaCl, 250 mM Immidazole pH 8.0, followed by size-exclusion chromatography (Superdex S200 16/60 GL; GE Healthcare) in 50 mM HEPES, pH 7.5, and 150 mM NaCl.

Mouse CD1d refolding and purification –mCD1d and β2M were separately expressed in *E. coli* and purified from inclusion bodies as reported for Qa-1a (48). The mCD1d-C12S/β2m complex was generated by refolding. First, 1 mg mCD1d and 2.4 mg mβ2m denatured inclusion bodies were loaded into two separate 1 ml syringes. Next, mCD1d and mβ2m were injected into 100 ml high-speed stirred cold refolding buffer (400 mM L-arginine, 100 mM Tris-HCl pH 8.0, 2 mM EDTA, 5 mM reduced glutathione, 0.5 mM oxidized glutathione, and 0.2 mM PMSF) through 26 gauge needles as close to the stirring bar as possible and incubated at 4 ˚C with medium-speed stirring. After 12 and 24 hours, additional 1mg mCD1d was added to the refolding reaction and continued to incubate until 72 hours under constant stirring. Finally, the refolding mixture was concentrated (Millipore Amicon 30K centrifugal filter) and purified by size exclusion chromatography on a Superdex S200 GL 10/300 in 50 mM HEPES pH 7.5, 150 mM NaCl. Refolded mCD1d-C9S/β2m complex was analyzed by SDS-PAGE.

CD1d-1B1 Fab complex formation and crystallization - Refolded or insect cell expressed mCD1d was incubated with equimolar amounts of recombinantly expressed 1B1 Fab (method?) or 1B1 Fab obtained by papain digestion for 4 hours at room temperature. The ternary mCD1d/1B1Fab complex was isolated by size exclusion chromatography using a Superdex S200 10/300 in 50 mM HEPES pH 7.5, 150 mM NaCl and further concentrated to 3-4 mg/ml in 10 mM HEPES pH 7.5, 30 mM NaCl for subsequent crystallization. Crystals were obtained in various combinations of CD1d and 1B1 Fab.

Crystallization and structure determination - The initial crystals of recombinant 1B1 Fab and refolded mCD1d complexes were grown as small plates by mixing 200 nl precipitant (100 mM MES pH 6.5, 12% (w/v) PEG 20K) with 200 nl protein solution at 22℃ using the sitting drop vapor diffusion method and the liquid handling robot Phoenix (Art Robbins Instruments). Other combinations such as insect cell mCD1d and papain digested 1B1 Fab also yielded crystals but of limited diffraction power. The diffraction-quality plate-like crystals were manually optimized and obtained in 80 mM MES pH 6.5, 8-10% (w/v) PEG 20K. Crystals were flash-cooled at 100 K in mother liquor containing 22% glycerol. Diffraction data were collected at the Stanford Synchrotron Radiation Laboratory (SSRL) beamline 9-2 and processed with HKL2000 (49). The 1B1 Fab/mCD1d crystal belong to space group $C222_1$ with unit cell parameters a=84.05 Å; b=160.96 Å; c=165.42 Å. The asymmetric unit contains one 1B1 Fab/mCD1d complex. The crystal structure was determined by molecular replacement using PHASER as part of the CCP4 suite (50,51). Protein coordinates from the mCD1d-iGb3 structure [PDB code 2Q7Y] (52) and the L363 Fab (PDB code 3UBX) (43) were used as the search models for mCD1d and the 1B1 Fab, respectively. The phased model was rebuilt into σ_A-weighted $2F_o–F_c$ and $F_o–F_c$ difference electron density maps using the program COOT (53) and refined in REFMAC5 (54). The complex structure was refined to 2.45 Å to an R_{cryst} and R_{free} of 21.0% and 24.7% respectively. The quality of the model was

examined with the program Molprobity (55). Data collection and refinement statistics are presented in Table 1.

Glycolipid loading and native isoelectric focusing (IEF) gel electrophoresis – For SPR or native IEF, 10 µl (~5 µg) of insect cell expressed mouse CD1d was loaded overnight with 6-10 times molar excess of either C24:1 sulfatide, bovine brain sulfatides, or GT1b (dissolved at 5-10 mg/ml in DMSO) in 100 mM HEPES pH 7.5, 150 mM NaCl without the addition of any detergents. Loading efficiency was analyzed via native IEF gel electrophoresis. For each protein-lipid complex, 4 µl solution were loaded onto a 6 well pH 5-8 native IEF gel and analyzed via the PhastSystem (GE Healthcare).

Surface plasmon resonance (SPR) studies. The real-time binding kinetics between 1B1 Fab and the CD1d-glycolipid complexes was analyzed by SPR using a Biacore T200 (Biacore, GE Healthcare) instrument. Briefly, insect cell expressed mCD1d protein containing a C-terminal birA-tag (LHHILDAQKMVWNHR) was enzymatically biotinylated and purified according to established methods (31,47). Biotinylated mCD1d was loaded with glycolipids overnight as reported above, and ≈ 400 RU of the individual mCD1d-glycolipd complexes were immobilized on a CAP sensor chip (GE Healthcare). A series of increasing concentrations (3-fold dilutions from 1.1 – 90 nM) of 1B1 Fab were passed over the immobilized CD1d-glycolipid complexes at 25 °C with a flow rate of 30 µl/min in a single cycle kinetic experiment. For background subtraction, flow channel 1 was similarly prepared but no protein was immobilized and the binding response of 1B1 Fab to flow channel 1 was subtracted from the other flow channel. The experiments were performed at least twice and kinetic parameters were calculated using a simple Langmuir 1:1 model in the BIA evaluation software

Cell free antigen presenting assay - APC free antigen presenting assay for stimulation of mouse iNKT cell hybridoma by soluble insect cell expressed mCD1d was carried out following published protocols (56,57). 96-well plates were coated with 1 µg of CD1d and incubated overnight at RT with 100 ng of glycolipids (1 µg/ml) in triplicates. Buffer was removed and indicated concentration of 1B1 Fab (0-100 µg) or 1B1 IgG (0-150 µg) in 50 µl or culture media added for 2 h at 37C. Hybridoma cells ($5x10^4$ of either Type I NKT 1.2 or Type II NKT XV19) in 50 µl culture media were added to each well and co-incubated with CD1d-glycolipid complexes overnight at 37˚C in a CO_2 incubator. IL-2 release in the APC free antigen-presenting assay was measured after 16 h of culture in a sandwich ELISA according to standard protocols to assess the extent to which 1B1 blocked both Type I and Type II NKT cell activation. As a negative control, the 1B1 Fab double mutant Y103K/I56S that lost mouse CD1d binding was generated.

Acknowledgements:
Use of the Stanford Synchrotron Radiation Lightsource, SLAC National Accelerator Laboratory, is supported by the U.S. Department of Energy, Office of Science, Office of Basic Energy Sciences under Contract No. DE-AC02-76SF00515. The SSRL Structural Molecular Biology Program is supported by the DOE Office of Biological and Environmental Research, and by the National Institutes of Health, National Institute of General Medical Sciences (including P41GM103393). The contents of this publication are solely the responsibility of the authors and do not necessarily represent the official views of NIGMS or NIH. This work was supported in part by the National Institute of Health grant AI137230 to DMZ.
The atomic coordinates and structure factors of the mCD1d-1B1-Fab complex have been deposited in the Protein Data Bank under accession number 6OOR, and the 1B1 sequences have been deposited in GenBank under accession code MK820936 (1B1LC) and MK820937 (1B1HC).

Conflict of interest: The authors declare that they have no conflict of interest with the contents of this article.

Author contributions: GY produced recombinant proteins and performed structural studies, JW generated recombinant proteins, performed SPR experiments, antibody sequencing, site-directed mutagenesis, and NKT cell activation assays. TM and SVC provided critical reagents. DMZ conceived the experiments, supervised the overall project and wrote the manuscript.

REFERENCES

1. Rossjohn, J., Gras, S., Miles, J. J., Turner, S. J., Godfrey, D. I., and McCluskey, J. (2015) T cell antigen receptor recognition of antigen-presenting molecules. *Annu Rev Immunol* **33**, 169-200
2. Denkberg, G., and Reiter, Y. (2006) Recombinant antibodies with T-cell receptor-like specificity: novel tools to study MHC class I presentation. *Autoimmun Rev* **5**, 252-257
3. Cohen, C. J., Denkberg, G., Lev, A., Epel, M., and Reiter, Y. (2003) Recombinant antibodies with MHC-restricted, peptide-specific, T-cell receptor-like specificity: new tools to study antigen presentation and TCR-peptide-MHC interactions. *J Mol Recognit* **16**, 324-332
4. Stewart-Jones, G., Wadle, A., Hombach, A., Shenderov, E., Held, G., Fischer, E., Kleber, S., Nuber, N., Stenner-Liewen, F., Bauer, S., McMichael, A., Knuth, A., Abken, H., Hombach, A. A., Cerundolo, V., Jones, E. Y., and Renner, C. (2009) Rational development of high-affinity T-cell receptor-like antibodies. *Proc Natl Acad Sci U S A* **106**, 5784-5788
5. Mareeva, T., Martinez-Hackert, E., and Sykulev, Y. (2008) How a T cell receptor-like antibody recognizes major histocompatibility complex-bound peptide. *J Biol Chem* **283**, 29053-29059
6. Dahan, R., Tabul, M., Chou, Y. K., Meza-Romero, R., Andrew, S., Ferro, A. J., Burrows, G. G., Offner, H., Vandenbark, A. A., and Reiter, Y. (2011) TCR-like antibodies distinguish conformational and functional differences in two- versus four-domain auto reactive MHC class II-peptide complexes. *Eur J Immunol* **41**, 1465-1479
7. Yu, K. O., Im, J. S., Illarionov, P. A., Ndonye, R. M., Howell, A. R., Besra, G. S., and Porcelli, S. A. (2007) Production and characterization of monoclonal antibodies against complexes of the NKT cell ligand alpha-galactosylceramide bound to mouse CD1d. *J Immunol Methods* **323**, 11-23
8. Denkberg, G., Stronge, V. S., Zahavi, E., Pittoni, P., Oren, R., Shepherd, D., Salio, M., McCarthy, C., Illarionov, P. A., van der Merwe, A., Besra, G. S., Dellabona, P., Casorati, G., Cerundolo, V., and Reiter, Y. (2008) Phage display-derived recombinant antibodies with TCR-like specificity against alpha-galactosylceramide and its analogues in complex with human CD1d molecules. *Eur J Immunol* **38**, 829-840
9. Brossay, L., Jullien, D., Cardell, S., Sydora, B. C., Burdin, N., Modlin, R. L., and Kronenberg, M. (1997) Mouse CD1 is mainly expressed on hemopoietic-derived cells. *J Immunol* **159**, 1216-1224
10. Bendelac, A., Savage, P. B., and Teyton, L. (2007) The Biology of NKT Cells. *Annu Rev Immunol* **25**, 297-336
11. Godfrey, D. I., MacDonald, H. R., Kronenberg, M., Smyth, M. J., and Van Kaer, L. (2004) NKT cells: what's in a name? *Nat Rev Immunol* **4**, 231-237
12. Godfrey, D. I., Rossjohn, J., and McCluskey, J. (2008) The fidelity, occasional promiscuity, and versatility of T cell receptor recognition. *Immunity* **28**, 304-314
13. Kawano, T., Cui, J., Koezuka, Y., Toura, I., Kaneko, Y., Motoki, K., Ueno, H., Nakagawa, R., Sato, H., Kondo, E., Koseki, H., and Taniguchi, M. (1997) CD1d-restricted and TCR-mediated activation of Vα14 NKT cells by glycosylceramides. *Science* **278**, 1626-1629
14. Blomqvist, M., Rhost, S., Teneberg, S., Lofbom, L., Osterbye, T., Brigl, M., Mansson, J. E., and Cardell, S. L. (2009) Multiple tissue-specific isoforms of sulfatide activate CD1d-restricted type II NKT cells. *European journal of immunology* **39**, 1726-1735

15. Gumperz, J. E., Roy, C., Makowska, A., Lum, D., Sugita, M., Podrebarac, T., Koezuka, Y., Porcelli, S. A., Cardell, S., Brenner, M. B., and Behar, S. M. (2000) Murine CD1d-restricted T cell recognition of cellular lipids. *Immunity* **12**, 211-221
16. Jahng, A., Maricic, I., Aguilera, C., Cardell, S., Halder, R. C., and Kumar, V. (2004) Prevention of autoimmunity by targeting a distinct, noninvariant CD1d-reactive T cell population reactive to sulfatide. *J Exp Med* **199**, 947-957
17. Tatituri, R. V., Watts, G. F., Bhowruth, V., Barton, N., Rothchild, A., Hsu, F. F., Almeida, C. F., Cox, L. R., Eggeling, L., Cardell, S., Rossjohn, J., Godfrey, D. I., Behar, S. M., Besra, G. S., Brenner, M. B., and Brigl, M. (2013) Recognition of microbial and mammalian phospholipid antigens by NKT cells with diverse TCRs. *Proc Natl Acad Sci U S A* **110**, 1827-1832
18. Le Nours, J., Praveena, T., Pellicci, D. G., Gherardin, N. A., Ross, F. J., Lim, R. T., Besra, G. S., Keshipeddy, S., Richardson, S. K., Howell, A. R., Gras, S., Godfrey, D. I., Rossjohn, J., and Uldrich, A. P. (2016) Atypical natural killer T-cell receptor recognition of CD1d-lipid antigens. *Nat Commun* **7**, 10570
19. Uldrich, A. P., Patel, O., Cameron, G., Pellicci, D. G., Day, E. B., Sullivan, L. C., Kyparissoudis, K., Kjer-Nielsen, L., Vivian, J. P., Cao, B., Brooks, A. G., Williams, S. J., Illarionov, P., Besra, G. S., Turner, S. J., Porcelli, S. A., McCluskey, J., Smyth, M. J., Rossjohn, J., and Godfrey, D. I. (2011) A semi-invariant Valpha10+ T cell antigen receptor defines a population of natural killer T cells with distinct glycolipid antigen-recognition properties. *Nat Immunol* **12**, 616-623
20. Zajonc, D. M., Maricic, I., Wu, D., Halder, R., Roy, K., Wong, C. H., Kumar, V., and Wilson, I. A. (2005) Structural basis for CD1d presentation of a sulfatide derived from myelin and its implications for autoimmunity. *The Journal of experimental medicine* **202**, 1517-1526
21. Zajonc, D. M., Cantu, C., Mattner, J., Zhou, D., Savage, P. B., Bendelac, A., Wilson, I. A., and Teyton, L. (2005) Structure and function of a potent agonist for the semi-invariant natural killer T cell receptor. *Nat Immunol* **8**, 810-818
22. Koch, M., Stronge, V. S., Shepherd, D., Gadola, S. D., Mathew, B., Ritter, G., Fersht, A. R., Besra, G. S., Schmidt, R. R., Jones, E. Y., and Cerundolo, V. (2005) The crystal structure of human CD1d with and without α-galactosylceramide. *Nat Immunol* **8**, 819-826
23. Zajonc, D. M. (2016) The CD1 family: serving lipid antigens to T cells since the Mesozoic era. *Immunogenetics* **68**, 561-576
24. Zajonc, D. M., and Girardi, E. (2015) Recognition of Microbial Glycolipids by Natural Killer T Cells. *Front Immunol* **6**, 400
25. Kinjo, Y., Illarionov, P., Vela, J. L., Pei, B., Girardi, E., Li, X., Li, Y., Imamura, M., Kaneko, Y., Okawara, A., Miyazaki, Y., Gomez-Velasco, A., Rogers, P., Dahesh, S., Uchiyama, S., Khurana, A., Kawahara, K., Yesilkaya, H., Andrew, P. W., Wong, C. H., Kawakami, K., Nizet, V., Besra, G. S., Tsuji, M., Zajonc, D. M., and Kronenberg, M. (2011) Invariant natural killer T cells recognize glycolipids from pathogenic Gram-positive bacteria. *Nat Immunol* **12**, 966-974
26. Girardi, E., Yu, E. D., Li, Y., Tarumoto, N., Pei, B., Wang, J., Illarionov, P., Kinjo, Y., Kronenberg, M., and Zajonc, D. M. (2011) Unique interplay between sugar and lipid in determining the antigenic potency of bacterial antigens for NKT cells. *PLoS Biol* **9**, e1001189
27. Dieude, M., Striegl, H., Tyznik, A. J., Wang, J., Behar, S. M., Piccirillo, C. A., Levine, J. S., Zajonc, D. M., and Rauch, J. (2011) Cardiolipin binds to CD1d and stimulates CD1d-restricted gammadelta T cells in the normal murine repertoire. *J Immunol* **186**, 4771-4781

28. Wang, J., Li, Y., Kinjo, Y., Mac, T. T., Gibson, D., Painter, G. F., Kronenberg, M., and Zajonc, D. M. (2010) Lipid binding orientation within CD1d affects recognition of Borrelia burgorferi antigens by NKT cells. *Proc Natl Acad Sci U S A* **107**, 1535-1540
29. Borg, N. A., Wun, K. S., Kjer-Nielsen, L., Wilce, M. C., Pellicci, D. G., Koh, R., Besra, G. S., Bharadwaj, M., Godfrey, D. I., McCluskey, J., and Rossjohn, J. (2007) CD1d-lipid-antigen recognition by the semi-invariant NKT T-cell receptor. *Nature* **448**, 44-49
30. Girardi, E., Maricic, I., Wang, J., Mac, T. T., Iyer, P., Kumar, V., and Zajonc, D. M. (2012) Type II natural killer T cells use features of both innate-like and conventional T cells to recognize sulfatide self antigens. *Nature immunology* **13**, 851-856
31. Li, Y., Girardi, E., Wang, J., Yu, E. D., Painter, G. F., Kronenberg, M., and Zajonc, D. M. (2010) The Vα14 invariant natural killer T cell TCR forces microbial glycolipids and CD1d into a conserved binding mode. *J Exp Med* **207**, 2383-2393
32. Patel, O., Pellicci, D. G., Gras, S., Sandoval-Romero, M. L., Uldrich, A. P., Mallevaey, T., Clarke, A. J., Le Nours, J., Theodossis, A., Cardell, S. L., Gapin, L., Godfrey, D. I., and Rossjohn, J. (2012) Recognition of CD1d-sulfatide mediated by a type II natural killer T cell antigen receptor. *Nat Immunol* **13**, 857-863
33. Pellicci, D. G., Patel, O., Kjer-Nielsen, L., Pang, S. S., Sullivan, L. C., Kyparissoudis, K., Brooks, A. G., Reid, H. H., Gras, S., Lucet, I. S., Koh, R., Smyth, M. J., Mallevaey, T., Matsuda, J. L., Gapin, L., McCluskey, J., Godfrey, D. I., and Rossjohn, J. (2009) Differential recognition of CD1d-alpha-galactosyl ceramide by the V beta 8.2 and V beta 7 semi-invariant NKT T cell receptors. *Immunity* **31**, 47-59
34. Aspeslagh, S., Li, Y., Yu, E. D., Pauwels, N., Trappeniers, M., Girardi, E., Decruy, T., Van Beneden, K., Venken, K., Drennan, M., Leybaert, L., Wang, J., Franck, R. W., Van Calenbergh, S., Zajonc, D. M., and Elewaut, D. (2011) Galactose-modified iNKT cell agonists stabilized by an induced fit of CD1d prevent tumour metastasis. *EMBO J* **30**, 2294-2305
35. Florence, W. C., Xia, C., Gordy, L. E., Chen, W., Zhang, Y., Scott-Browne, J., Kinjo, Y., Yu, K. O., Keshipeddy, S., Pellicci, D. G., Patel, O., Kjer-Nielsen, L., McCluskey, J., Godfrey, D. I., Rossjohn, J., Richardson, S. K., Porcelli, S. A., Howell, A. R., Hayakawa, K., Gapin, L., Zajonc, D. M., Wang, P. G., and Joyce, S. (2009) Adaptability of the semi-invariant natural killer T-cell receptor towards structurally diverse CD1d-restricted ligands. *EMBO J* **28**, 3781
36. Wun, K. S., Cameron, G., Patel, O., Pang, S. S., Pellicci, D. G., Sullivan, L. C., Keshipeddy, S., Young, M. H., Uldrich, A. P., Thakur, M. S., Richardson, S. K., Howell, A. R., Illarionov, P. A., Brooks, A. G., Besra, G. S., McCluskey, J., Gapin, L., Porcelli, S. A., Godfrey, D. I., and Rossjohn, J. (2011) A molecular basis for the exquisite CD1d-restricted antigen specificity and functional responses of natural killer T cells. *Immunity* **34**, 327-339
37. Girardi, E., and Zajonc, D. M. (2012) Molecular basis of lipid antigen presentation by CD1d and recognition by natural killer T cells. *Immunol Rev* **250**, 167-179
38. Girardi, E., Wang, J., and Zajonc, D. M. (2016) Structure of an alpha-Helical Peptide and Lipopeptide Bound to the Nonclassical Major Histocompatibility Complex (MHC) Class I Molecule CD1d. *J Biol Chem* **291**, 10677-10683
39. Ito, Y., Vela, J. L., Matsumura, F., Hoshino, H., Tyznik, A., Lee, H., Girardi, E., Zajonc, D. M., Liddington, R., Kobayashi, M., Bao, X., Bugaytsova, J., Boren, T., Jin, R., Zong, Y., Seeberger, P. H., Nakayama, J., Kronenberg, M., and Fukuda, M. (2013) Helicobacter pylori cholesteryl alpha-glucosides contribute to its pathogenicity and immune response by natural killer T cells. *PLoS One* **8**, e78191
40. Guillaume, J., Wang, J., Janssens, J., Remesh, S. G., Risseeuw, M. D. P., Decruy, T., Froeyen, M., Elewaut, D., Zajonc, D. M., and Calenbergh, S. V. (2017)

Galactosylsphingamides: new alpha-GalCer analogues to probe the F'-pocket of CD1d. *Sci Rep* **7**, 4276

41. Wang, J., Guillaume, J., Pauwels, N., Van Calenbergh, S., Van Rhijn, I., and Zajonc, D. M. (2012) Crystal structures of bovine CD1d reveal altered alphaGalCer presentation and a restricted A' pocket unable to bind long-chain glycolipids. *PLoS One* **7**, e47989
42. Wu, D., Xing, G. W., Poles, M. A., Horowitz, A., Kinjo, Y., Sullivan, B., Bodmer-Narkevitch, V., Plettenburg, O., Kronenberg, M., Tsuji, M., Ho, D. D., and Wong, C. H. (2005) Bacterial glycolipids and analogs as antigens for CD1d-restricted NKT cells. *Proc Natl Acad Sci U S A* **102**, 1351-1356
43. Yu, E. D., Girardi, E., Wang, J., Mac, T. T., Yu, K. O., Van Calenbergh, S., Porcelli, S. A., and Zajonc, D. M. (2012) Structural basis for the recognition of C20:2-alphaGalCer by the invariant natural killer T cell receptor-like antibody L363. *The Journal of biological chemistry* **287**, 1269-1278
44. Gilliland, L. K., Norris, N. A., Marquardt, H., Tsu, T. T., Hayden, M. S., Neubauer, M. G., Yelton, D. E., Mittler, R. S., and Ledbetter, J. A. (1996) Rapid and reliable cloning of antibody variable regions and generation of recombinant single chain antibody fragments. *Tissue Antigens* **47**, 1-20
45. Brady, J. L., Corbett, A. J., McKenzie, B. S., and Lew, A. M. (2006) Rapid specific amplification of rat antibody cDNA from nine hybridomas in the presence of myeloma light chains. *J Immunol Methods* **315**, 61-67
46. Lefranc, M. P., Giudicelli, V., Ginestoux, C., Bodmer, J., Muller, W., Bontrop, R., Lemaitre, M., Malik, A., Barbie, V., and Chaume, D. (1999) IMGT, the international ImMunoGeneTics database. *Nucleic acids research* **27**, 209-212
47. Hava, D. L., Brigl, M., van den Elzen, P., Zajonc, D. M., Wilson, I. A., and Brenner, M. B. (2005) CD1 assembly and the formation of CD1-antigen complexes. *Curr Opin Immunol* **17**, 88-94
48. Ying, G., Wang, J., Kumar, V., and Zajonc, D. M. (2017) Crystal structure of Qa-1a with bound Qa-1 determinant modifier peptide. *PLoS One* **12**, e0182296
49. Otwinowski, Z., and Minor, W. (1997) Processing of X-ray diffraction data collected in oscillation mode. *Methods Enzymol.* **276**, 307-326
50. McCoy, A. J., Grosse-Kunstleve, R. W., Storoni, L. C., and Read, R. J. (2005) Likelihood-enhanced fast translation functions. *Acta Crystallogr.* **D61**, 458-464
51. CCP4. (1994) Collaborative Computational Project, Number 4. The CCP4 Suite: Programs for Protein Crystallography. *Acta Crystallogr.* **D50**, 760-763
52. Zajonc, D. M., Savage, P. B., Bendelac, A., Wilson, I. A., and Teyton, L. (2008) Crystal structures of mouse CD1d-iGb3 complex and its cognate Vα14 T cell receptor suggest a model for dual recognition of foreign and self glycolipids. *J Mol Biol* **377**, 1104-1116
53. Emsley, P., and Cowtan, K. (2004) Coot: model-building tools for molecular graphics. *Acta Crystallogr D Biol Crystallogr* **60**, 2126-2132
54. Murshudov, G. N., Vagin, A. A., and Dodson, E. J. (1997) Refinement of macromolecular structures by the maximum likelihood method. *Acta Crystallogr.* **D53**, 240-255
55. Lovell, S. C., Davis, I. W., Arendall, W. B., 3rd, de Bakker, P. I., Word, J. M., Prisant, M. G., Richardson, J. S., and Richardson, D. C. (2003) Structure validation by Cα geometry: ϕ,ψ and Cβ deviation. *Proteins* **50**, 437-450
56. Kinjo, Y., Wu, D., Kim, G., Xing, G. W., Poles, M. A., Ho, D. D., Tsuji, M., Kawahara, K., Wong, C. H., and Kronenberg, M. (2005) Recognition of bacterial glycosphingolipids by natural killer T cells. *Nature* **434**, 520-525
57. Kinjo, Y., Tupin, E., Wu, D., Fujio, M., Garcia-Navarro, R., Benhnia, M. R., Zajonc, D. M., Ben-Menachem, G., Ainge, G. D., Painter, G. F., Khurana, A., Hoebe, K., Behar, S.

M., Beutler, B., Wilson, I. A., Tsuji, M., Sellati, T. J., Wong, C. H., and Kronenberg, M. (2006) Natural killer T cells recognize diacylglycerol antigens from pathogenic bacteria. *Nat Immunol* **7**, 978-986

58. Krissinel, E., and Henrick, K. (2007) Inference of macromolecular assemblies from crystalline state. *J Mol Biol* **372**, 774-797

TABLES

Table 1. Data collection and refinement statistics

Data collection statistics	mCD1d/1B1 complex
PDB ID	
Space group	$C222_1$
Cell dimension	
a, *b*, *c*, (Å)	84.1, 161.0, 165.4
α=β= γ (°)	90.00
Resolution range (Å)	40.0 -2.45
[outer shell]	(2.54-2.45)
No. of unique reflections	41,732 (4,082)
R_{meas} (%)	8.1 (62.0)
R_{pim} (%)	3.1 (25.0)
Multiplicity	6.6 (5.9)
Average I/σ	19.1 (1.8)
Completeness (%)	99.7 (98.5)
Refinement statistics	
No. atoms	6,530
Protein	6,337
Water	141
Sodium	4
Ligand	48
Ramachandran plot (%)	
Favored	95.2
Allowed	99.7
Outliers	0.3
R.m.s. deviations	
Bonds (Å)	0.005
Angles (°)	1.37
B-factors (Å^2)	
Protein	59.6
Water	49.1
Sodium	50.6
Ligand	52.8
R factor (%)	20.9
R_{free} (%)	24.4

Table 2. Comparison of Fab/TCR-mCD1d-glycolipid contacts

Individual buried surface areas within the ternary complexes (BSA in Å^2)	**1B1-endogenous lipid/ mCD1d[a]**	**L363-C20:2-αGalCer/ mCD1d[b]**	**Vα14Vβ8.2TCR-C20:2-αGalCer - mCD1d[c]**
mCD1d	610	710	680
glycolipid	110	160	150
Fab VL/TCR Vα	50	410	660
Fab VH/TCR Vβ	580	470	170
Fab/TCR - CD1d	1,430	1,610	1,600

[a,b,c] Values are calculated using PISA (58). [b,c] Values from (43).

Table 3. Atomic contacts in the mCD1d-1B1-Fab complex

CDR	1B1	Endogenous lipid	Bonds
H3	Leu106	UNK1 C8	VDW
	Gly105	UNK1 C12	VDW
	Tyr104	UNK1 C16	VDW
CDR	**1B1**	**mCD1d**	**Bonds**
L1	Tyr31	Glu83	VDW
H2	Asp55	Lys148	Salt bridge
		Lys148	H bond
	Ile56	Lys148	VDW
		Val149	VDW
		Leu145	VDW
H3	Tyr103	Ala152	VDW
		Asp153	VDW
	Tyr104	Asp153	VDW
	Gly105	Asp153	H bond
		Leu150	VDW
		Asp80	VDW
		Val149	VDW
	Leu106	Asp80	H bond
		Leu84	VDW
		Leu150	VDW
		Pro146	VDW
		Val149	VDW
	Leu107	Val149	VDW
		Asp80	VDW
		Glu83	VDW
	Leu108	Val149	VDW
	Arg109	Asp80	Salt bridge

The molecular interactions within the complex were analyzed using the program CONTACT (CCP4, 1994). The distance cut-offs used were 4 Å (van der Waals interactions, VDW), 3.5 Å (hydrogen bonds) and 4.5 Å (salt bridges).

FIGURE LEGENDS

FIGURE 1. *Structure of the mCD1d/ 1B1 Fab complex.* (A) Cartoon representation of 1B1 Fab (L chain in green, H chain in orange) bound across the α1 and α2 helices of mCD1d. (B) Interactions between 1B1 H3 region and the binding groove residues of CD1d. (C) 1B1 H2 interactions with CD1d. (D) Light chain contacts with CD1d are restricted to L1, without direct polar interactions. (E) Footprint of 1B1 Fab on CD1d (grey molecular surface) colored by H and L chain. Heavy chain forms the majority of contacts, while the L chain barely contacts Arg79 (R79) and Glu83 (E83). Binding footprint of 1B1 is centered above the F′ pocket of CD1d.

FIGURE 2. CDR *H3 of 1B1 contacts the spacer lipid.* (A) Three spacer molecules (yellow sticks with FoFc electron density map contoured at 3σ) are bound in the CD1d binding groove (grey molecular surface, cut open). H3 residues as orange sticks with vdW interactions with the spacer molecule as black dashed lines. Note how deep Leu106 of H3 is inserted into the F′ pocket of CD1d. (B) Molecular model with sulfatide occupying the CD1d binding groove shows close contacts between the galactose headgroup and the H3 loop. (C) native IEF gel of insect cell expressed mCD1d (lane 1, band at 0) with fully loaded bovine brain sulfatides (lane 2, band at -1) or GT1b (lane 3, band at -3). (D) SPR sensorgram (single cycle kinetics) of 1B1 Fab to immobilized CD1d presenting the different CD1d-glycolipid complexes shown in panel C. Binding kinetics are not influenced by the nature of the lipid. Kinetic values are indicated in each panel. (E) Binding response of 100 nM of wildtype 1B1 Fab or the 1B1 Fab Y103K/I56S double mutant to either human or mouse CD1d.

FIGURE 3. *Comparison between 1B1 Fab and Vα14Vβ8.2 TCR binding to CD1d.* (A) Similar view as in Figure 2A illustrating how deep H3 (orange) of 1B1 is inserted into the F′ pocket of CD1d compared to CDR3α (cyan) of the TCR. PDB ID 3HE6 is shown for the CD1d-αGalCer-TCR complex, with the 1B1 position overlayed. The ligand αGSA[26,P5*p*] is superposed on αGalCer and reveals close contacts with Leu106H of 1B1. Hydrophobic fingers $L106_H$ and Leu99α are shown. (B) The different binding mode of both H3 and CDR3α lead to a different side chain orientation of the CD1d F′ pocket lining residues. CD1d residues from the 1B1 complex as grey sticks and those from the TCR complex as cyan sticks. (C) The long H3 loop prevents the F′ roof closure of CD1d, as it penetrates into the F′ pocket, while CDR3α of the TCR sits above the F′ pocket and binds above the closed F′ roof (D).

FIGURE 4. *1B1 blocks both Type I and Type II NKT cell activation.* (A) NKT cell hybridoma activation assay using CD1d coated plates presenting the lipids αGalCer, αGSA[26P5*p*], and sulfatide. Addition of 1B1 Fab (top row) or 1B1 IgG (bottom row) reduces IL-2 production in a dose dependent manner (black bars). An engineered 1B1 Fab mutant that cannot bind to mCD1d or an isotype control IgG do not block NKT cell activation (grey bars). Middle columns indicate that 1B1 Fab is not able to block NKT cell activation by αGSA[26P5*p*], while 1B1 IgG retains blocking, albeit at a slightly higher IgG concentration. Each experiment has been performed twice with each measurement in triplicate. Standard deviation is shown with error bars. (B) CD1d binding footprint of the individual TCRs (2C12 and XV19) and 1B1 Fab are shown for comparison. Residues Ser76 (S76) and Arg79 (R79) are shared contact residues of CD1d and labeled.

FIGURES

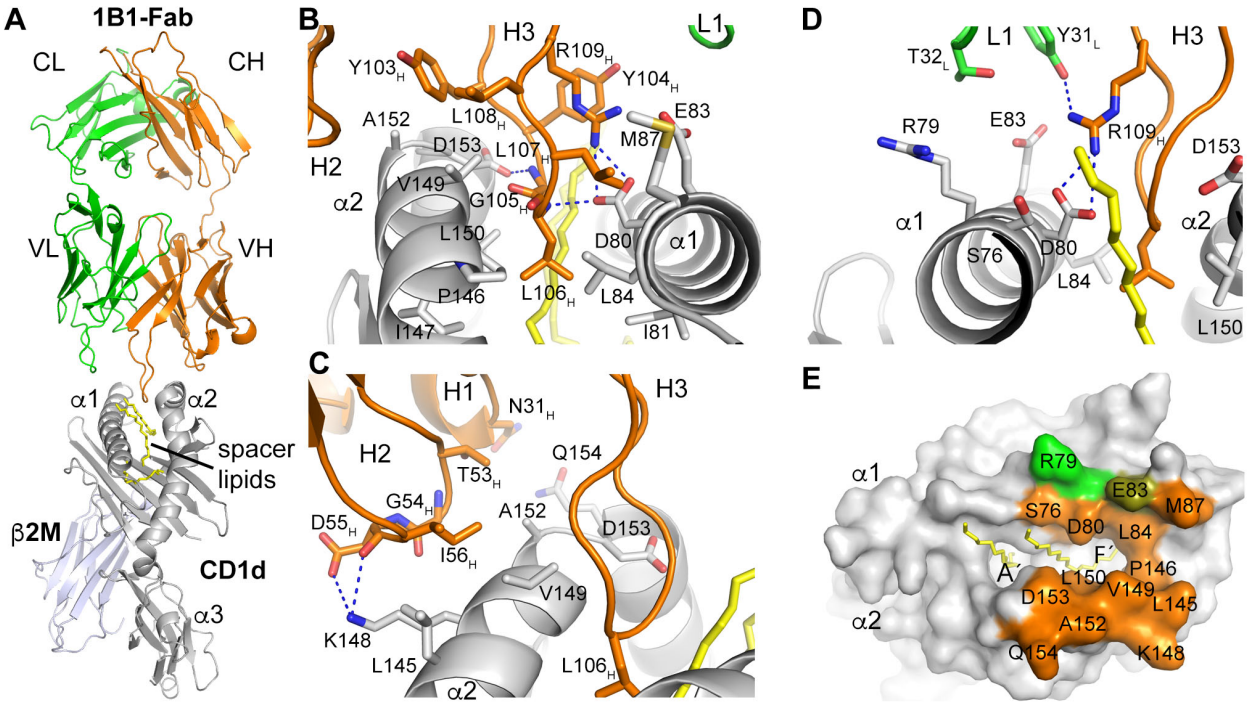

Figure 1

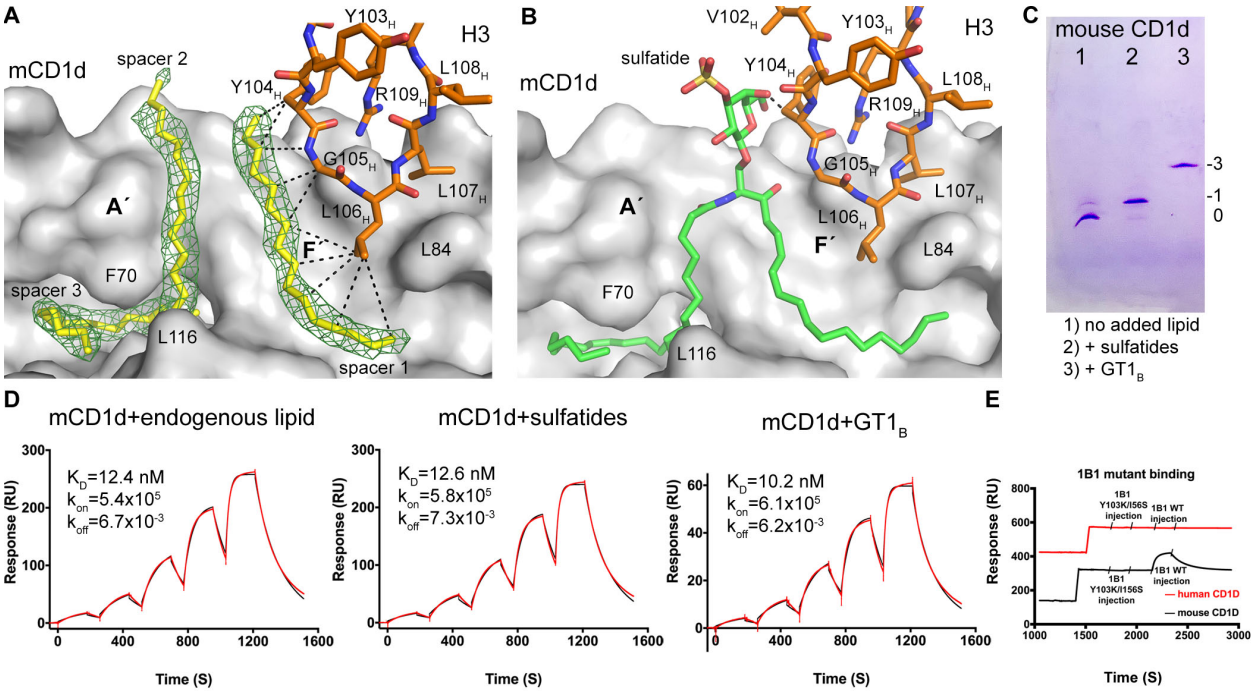
A
mCD1d
spacer 2
Y103H
H3
Y104H
L108H
R109H
G105H
L107H
L106H
A´
F
L84
F70
spacer 3
L116
spacer 1
B
V102H
Y103H
H3
sulfatide
Y104H
mCD1d
L108H
R109H
G105H
L107H
A´
L106H
F´
L84
F70
L116
C
mouse CD1d
1 2 3
-3
-1
0
1) no added lipid
2) + sulfatides
3) + GT1B
D
mCD1d+endogenous lipid
KD=12.4 nM
kon=5.4x10^5
koff=6.7x10^-3
mCD1d+sulfatides
KD=12.6 nM
kon=5.8x10^5
koff=7.3x10^-3
mCD1d+GT1B
KD=10.2 nM
kon=6.1x10^5
koff=6.2x10^-3
Response (RU)
Time (S)
E
1B1 mutant binding
1B1 Y103K/I56S injection
1B1 WT injection
1B1 Y103K/I156S injection
human CD1D
mouse CD1D
Response (RU)
Time (S)

Figure 2

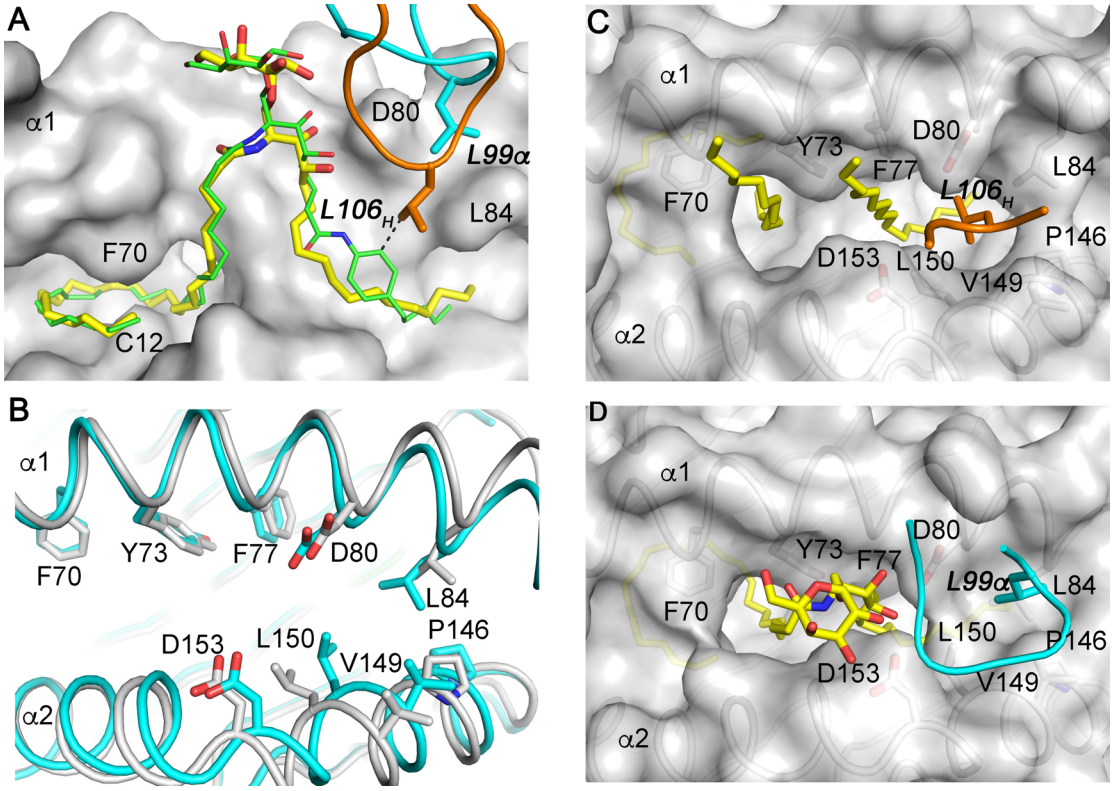
A
α1
D80
L99α
L106H
L84
F70
C12
B
α1
Y73
F77
D80
F70
L84
P146
D153
L150
V149
α2
C
α1
D80
Y73
F77
L84
L106H
F70
P146
D153
L150
V149
α2
D
α1
D80
Y73
F77
L99α
L84
F70
L150
P146
D153
V149
α2

Figure 3

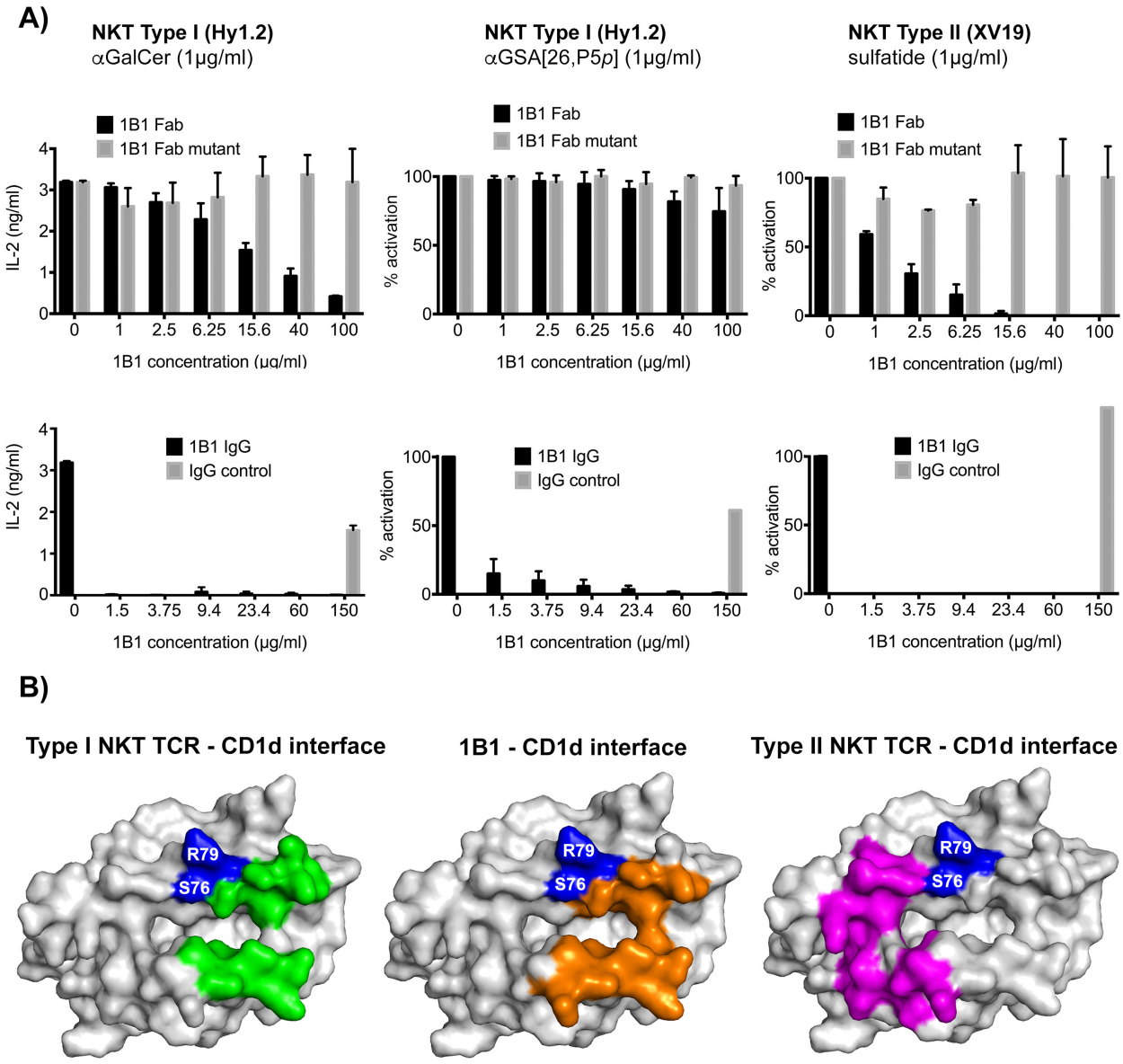
A)
NKT Type I (Hy1.2)
αGalCer (1μg/ml)
NKT Type I (Hy1.2)
αGSA[26,P5p] (1μg/ml)
NKT Type II (XV19)
sulfatide (1μg/ml)
1B1 Fab
1B1 Fab mutant
IL-2 (ng/ml)
% activation
0 1 2.5 6.25 15.6 40 100
1B1 concentration (μg/ml)
1B1 IgG
IgG control
0 1.5 3.75 9.4 23.4 60 150
B)
Type I NKT TCR - CD1d interface
1B1 - CD1d interface
Type II NKT TCR - CD1d interface
R79
S76

Figure 4